

# LANDMARK EXTRACTION FROM LEAVES WITH PALMATE VENATION

## *Application to Grape*

Raffi Enficiaud and Sofiène Mouine

INRIA Paris-Rocquencourt - IMEDIA, Domaine de Voluceau - Rocquencourt - B.P. 105, 78153 Le Chesnay, France

**Keywords:** Plant identification, Venation extraction, Mathematical morphology, Computational botany.

**Abstract:** The growing interest of Content Base Image Retrieval techniques in the context of plant identification requires the development of appropriate features. A considerable amount of information about the taxonomic identity of a plant is contained in its leaves, and most of the botanical expertise uses jointly the contour and the venation network. The current work focuses principally on the extraction of the venation network, the base and secondary landmarks of leaves with uncluttered background, assuming only their structure as palmate. Morphological operators are used to extract a first approximation of the venation network, which is then filtered by a voting scheme and reconstructed using a connected component like algorithm. The base point and the primary veins are then extracted with an accuracy of 100%, which allows identification of the lobes and the measurement their relative length.

## 1 INTRODUCTION

The wine industry is ruled by laws on exploitation and trade. Identifying the exact type of vine is a critical issue for people involved in its exploitation. A wide variety of actors is concerned by vine identification, but only a few of them has knowledge in botany. This is in contrast with the difficulty of the task, since the identification is almost solely achievable by experts in this specific field. The difficulty of the identification explains the growing interest in automated procedures, such as *Content Based Image Retrieval* (CBIR) techniques, which application in this field is relatively new and has shown to provide promising performances. Aside from any technical feasibility issue, CBIR endows non-expert users with fast retrieval, similarity and browsing methods, which potentially could solve the task of identification without the need for external expertise. A considerable amount of information about the taxonomic identity of a plant is contained in its leaves. In addition to their discriminative power, leaves are parts of plants that are observable at almost any stage of maturity. CBIR was successful in classifying Orchid species (Coutaud et al., 2009) from scan of their leaves and using common colour and texture descriptors. In this paper, we present a method for extracting meaningful landmarks from the leaves, only under the assumption of a *palmate* struc-

ture, a family to which the grapes belong. These landmarks are chosen to be as close as possible to the existing botanical expertise, in order to develop feature extraction techniques that remain humanly interpretable. To the authors knowledge, the specific task of grapes identification from their leaves is addressed exclusively in the botany community. Hence, no particular reference nor ground truth are available for evaluations. In the botany community, a lot of work has been achieved so far and the current state of knowledge is constantly renewed. The reader is referred to (OIV expert group “Vine selection”, 2009), which describes the identification cues for wide variety of grapes. Many of these rely on the general appearance of the leaf (eg. the number of lobes, the overall shape of the blade.) Others are defined directly on the venations (eg. length and relative angles), or on a combination of the boundary of the blade and the venation (eg. length and width of the tooth.) The authors of (Park et al., 2006) extract the venation pattern of the leaves. Combined with the shape (Nam et al., 2008), the venation improves the accuracy of the identification. The paper is organized as follows. Section 2 presents the general settings. Section 3 describes a method for extracting the venation network. These results are used for reconstructing the venation network and detecting the base point in Section 4. Section 5 concludes and provides directions for future work.

## 2 GENERAL SETTINGS

Our database contains 20 varieties of grapes, each of which containing 19 images. Each image contains one leaf on an uncluttered background. The grape leaves are all *palmate*, which means that several *primary* veins split from the *petiole* (leaf stalk). From primary veins then start secondary veins at bifurcation points. In the image plane, the location where the petiole joins the blade is considered as the *base* point. The leaves have very different aspects even within a class, as they are non-rigid objects and their planarity is not guaranteed. They also may or not have lobes that create local occlusions. The venation seems to be the proper element on which we can normalize the measurements. The settings make the segmentation of the blade straightforward: a chromatic threshold in the *GHLS* (Levkowitz and Herman, 1993) colour space provides very accurate results. Some meaningful information cannot be retrieved from the contour of the leaf alone. This is the case for instance for the lobes, their number and their apexes. Indeed the tooth of the blade is of the same amplitude for the apex and its surroundings, which makes the apex of the lobe hardly distinguishable.

## 3 VENATION EXTRACTION

The veins are locally linear structures that have a contrast with the blade. They may be either brighter or darker than the blade, depending on the variety, and the contrast level is not known a priori. These properties make mathematical morphology operators, especially top-hat and opening with line structuring elements (SE) following (Zana and Klein, 2001) ideal candidates for extracting these structures.

### 3.1 Morphological Processing

We denote  $S_\ell^\alpha$  the segment SE of length  $\ell$  and orientation  $\alpha$ . We also denote  $\gamma_{S_\ell^\alpha}$  the morphological opening using the SE  $S_\ell^\alpha$ . Given a particular orientation  $\alpha$ , we want to extract the meaningful segments with direction  $\alpha$  from the image. We first extract the elements that cannot fit into a line of length  $\ell_1$  and of direction  $\alpha^\perp = \alpha + \pi/2$  with a morphological *top-hat*, in order to extract the structures having a contrast along  $\alpha^\perp$ . We then apply a morphological opening using  $S_{\ell_2}^\alpha$  to extract the segments of direction  $\alpha$  and of length at least  $\ell_2$ . Efficient implementation of directional filtering exists (eg.(Soille and Talbot, 2001).)

The processing is performed on the luminance channel. In our experiments, we considered 12 direc-

tions uniformly distributed on  $[0, \pi[$ . The sizes of the SE play a major role in the detection of the venation. Ideally  $\ell_1$  should be of the magnitude of the thickness of the leaves, and  $\ell_2$  should be wide enough to filter out small structures that cannot be associated to segments of interest. However even with finely tuned parameters, the retrieved veins will, in all cases, be disconnected due to first, the curvature and bifurcation points of the venation network and second, to the angular resolution. Rather, we consider this step as an initial filtering of the venation with a certain amount of false detection, that we further use to recover the base and the primary veins. Although the SE are straight lines, the thickness of the veins allows to consider slightly curved approximations, and we approximate the connected components (CC) of  $\text{im}_{\text{filt}}$  with a 2-polynomial using a linear regression. The 2-polynomial representation allows several computations in closed form (intersection, length...) that are easily expressed, and accommodates the curvature of the detections.

### 3.2 Meaningful Veins

The number of false alarms produced by the previous processing is often high, and we propose a method for keeping the *meaningful* polynomials. As the scale of the leaf is not a priori known, no parameter on the size of the polynomials should be used. We denote by  $s_k$  the segment indexed by  $k \in \{(i, \alpha), (j, \theta)\}$  and  $s_i^\alpha \cap s_j^\theta$  the intersection points of polynomials  $s_i^\alpha$  and  $s_j^\theta$ . Alg.1 favours the polynomials that are on the path of other polynomials. Also, the longer the polynomials, the higher the associated vote. The purpose is to reduce the number of entities of interest in each direction, for instance by keeping the  $n$  highest votes in

---

**Algorithm 1:** Meaningful veins - Pseudo-code.

---

**Data:**  $l_i^\alpha$  input CC in each direction indexed by  $i$  and  $\alpha$ ,  $n_1, n_2$ : complexity parameters,  $n$ : number of meaningful detection per  $\alpha$

**Result:**  $o^\alpha$ : detected meaningful veins

```

1 forall the  $\alpha$  do
2    $s^\alpha \leftarrow$  polynomials  $l_i^\alpha$  sorted by decreasing
   length;
3  $v_i^\alpha \leftarrow 0$ ;
4 forall the  $\alpha, \theta, \theta \neq \alpha, i \in \mathbb{N}_{n_1}^*, j \in \mathbb{N}_{n_2}^*$  do
5   forall the  $t \in s_i^\alpha \cap s_j^\theta, p \in t,$ 
    $(k, k') \in \{(i, \alpha), (j, \theta)\}^2, k \neq k'$  do
6     if  $p \in s_k$  then  $v_k \leftarrow v_k + 1$ ;
7 forall the  $\alpha$  do
8    $o^\alpha \leftarrow$  first  $n$  element of  $s^\alpha$  sorted by  $v^\alpha$ ;
```

---

each direction<sup>1</sup>. Due to the angular resolution, some directions do not have any relevant polynomials but still are in the final set of detected segments (see Fig.1 & 3, first row.) This issue will be addressed in the next section.

## 4 BASE DETECTION

Since the venation network is palmate, we can argue that the base point is at the intersection of the primary veins. We hence compute the intersection points for each pair of candidate polynomials of Alg.1, and keep the points that either lie within the range used for the approximation of both polynomials, or are close to it. In fact, keeping only intersection points lying within the range of approximation filters out relevant intersection points, explained by the fact that the base point is often a large area of venation, which makes the directional top-hat miss the zone. In our experiments, we considered intersection points that are not further away than 5% of the length of the candidate vein. We associate to each intersection  $\mathbf{x}_k$  a weight  $\mathbf{w}_k$  that favours angles close to  $\pi/2$  at the intersection point between the two involved polynomials.

Given the intersections, we then use the mean-shift (MS) (Comanicu and Meer, 2002) algorithm to find the local maximum density locations, which we consider as being candidates for the base of the leaf. Using the normal density estimates, the update rule yields

$$\mathbf{y}_{i+1} = \frac{\sum_{k \in \mathcal{N}_x} \mathbf{x}_k \cdot \mathbf{w}_k \cdot \exp\left(\left\|\frac{\mathbf{y}_i - \mathbf{x}_k}{h}\right\|^2\right)}{\sum_{k \in \mathcal{N}_x} \mathbf{w}_k \cdot \exp\left(\left\|\frac{\mathbf{y}_i - \mathbf{x}_k}{h}\right\|^2\right)} \quad (1)$$

where  $\mathcal{N}_x$  stands for an appropriate neighbourhood of the intersection point  $\mathbf{x}$  weighted by  $\mathbf{w}$ . In our experiments, we took the neighbourhood as being a ball of radius 1% of the image size. The result of the MS algorithm is a set of *local modes*, that we cluster together as explained in (Comanicu and Meer, 2002), resulting in a set of candidates  $\mathcal{C}$ . Selecting the base as the mode with highest density (denominator of Equ.1) provides 99.74% of correct results. However, in this setting, some polynomials may appear with high similarity at different orientations, each of which creating intersection points. Moreover, the number of votes/intersections grows quadratically in the number of polynomials. This is why we believe that relying on the density alone will not behave correctly for other databases and will be sensitive to noise.

<sup>1</sup>in our experiments, we took  $n_1 = 10$ ,  $n_2 = 5$  and  $n = 3$ .

## 4.1 Network Reconstruction

As mentioned, the candidate venation network computed in §3.2 is disconnected. Moreover, some polynomials are redundant as they were detected at close angular directions. We consider a path as a sequence of 2-polynomials along with their boundary. The complete algorithm proceeds in two similar steps: first it prunes, merges and splits intersecting polynomials into an initial set of paths  $\mathcal{P}$ . It then merges this set of paths with *close* and compatible orientations boundaries. The algorithm starts by sorting the initial set of polynomials  $\mathcal{S}$  by decreasing length. It then proceeds in a way similar to a region growing by hill climbing, with the difference that it may create new polynomials during the growing, which should then be correctly handled. A FIFO queue  $\mathbf{c}$  is initialized with the first element of  $\mathcal{S}$ . Two other queues  $\mathbf{p}, \mathbf{g}$ , used respectively for the current path, and the pruned polynomials, and a priority queue  $\mathbf{q}$  are also initialized. For each popped-out element  $e$  of  $\mathbf{c}$ , all polynomials  $t$  in  $\mathcal{S}$ , but not in  $\mathbf{p}$ ,  $\mathbf{c}$  or  $\mathbf{g}$ , and intersecting  $e$  within their respective boundary and with an angle lower than  $\pi/12$ , are selected. Let's call  $i$  the intersection of  $t$  and  $e$  meeting these constraints. If the boundaries of  $t$  are completely included in those of  $e$ , then  $t$  is targeted for pruning and added into  $\mathbf{g}$ . Otherwise,  $e$  and  $t$  are split at their intersection  $i$ . From the four parts obtained, the longest configuration is kept, yielding left and right polynomials  $l_{t,c}, r_{t,c}$ . The new polynomial  $l_{t,c} \cup r_{t,c}$  is inserted into  $\mathbf{q}$ . After all candidates  $t$  have been tested, either  $\mathbf{q}$  is empty, in which case  $e$  is added to the current reconstructed path  $\mathbf{p}$ , or  $\mathbf{q}$  contains new polynomials not in  $\mathcal{S}$ . In that case, for the  $t$  generating the longest new polynomial,  $e$  and  $t$  are both removed from  $\mathcal{S}$ , and  $l_{t,c}$  and  $r_{t,c}$  are added both into  $\mathcal{S}$  and  $\mathbf{c}$  (region growing). Finally, when no growing is possible,  $\mathcal{P} = \mathcal{P} \cup \mathbf{p}$  and  $\mathcal{S} = \mathcal{S} - \mathbf{p} \cup \mathbf{g}$ .

For the second part of the reconstruction, instead of considering intersecting polynomials, paths not distant from more than  $2 \times \mathcal{R}$ , with  $\mathcal{R}$  the radius of the kernel used in Equ.1 are considered. Indeed, polynomials separated by at most  $2 \times \mathcal{R}$  will get selected by a base candidate (see next section).

## 4.2 Base Selection

For each of the MS candidates  $c \in \mathcal{C}$ , we select the subset  $Q_c$  of paths from  $\mathcal{P}$  such that  $Q_c = \{p \in \mathcal{P}, \exists p_i \in p \text{ st. } d(p_i, c) < \mathcal{R}\}$ , which amounts to solve the roots of a 3-polynomial. We then consider the base point  $\mathbf{B}$  as being

$$\mathbf{B} = \arg \max_{c \in \mathcal{C}} \sum_{p \in Q_c} \text{length}(p)$$

With the proposed method, the achieved accuracy in the detection of the base is 100% for the specified database, even for leaves with defects (see Fig.4.) We should note that the detection of the base point is of principal interest, since the structure of the venation network is hierarchical and rooted on the base point. Hence its detection should also be considered for joining disconnected veins. Indeed, prematurely linking some venation paths together irremediably degrades the accuracy of the venation structure on the whole database.

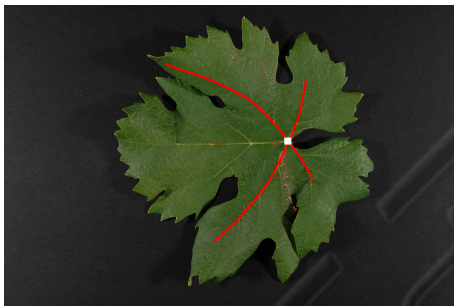
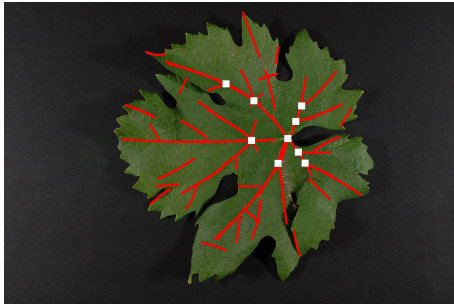


Figure 1: “Servant” variety. Top: filtered venation network (red) and MS candidates  $\mathcal{C}$  (white). Bottom: detection of the base (white) and associated primary veins  $\mathcal{Q}_{\mathbf{B}}$  (red).

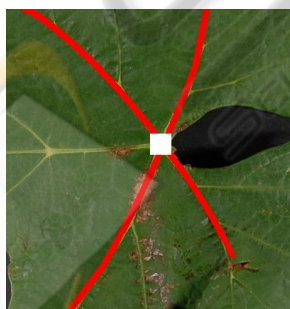


Figure 2: “Servant” variety: zoom over the base area. The damage prevents from linking the base to the horizontal path.

### 4.3 Other Landmarks

From the reconstructed primary venation network  $\mathcal{P}$ , the extremities of the lobes are easily extracted by

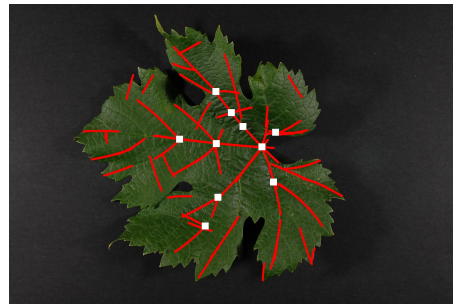


Figure 3: “Merlot” variety. See Fig.1 for legend.

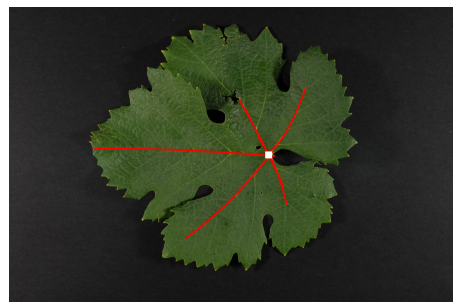
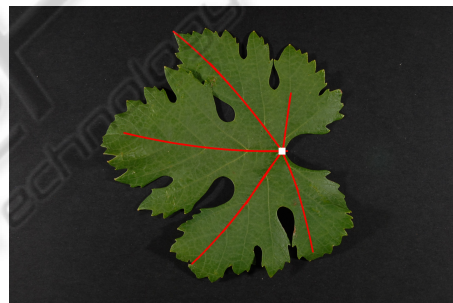


Figure 4: More results from “Servant” variety. See Fig.1 (bottom) for legend.

extrapolating the path. We used a linear extrapolation with direction given by the mean of the tangent of the 2-polynomials close to their boundary. This is explained by the fact that the 2-polynomial representation is accurate only within the CC used for its regression, and may strongly diverge outside the CC. We also recall that the leaves are not assumed to be planar. The other base candidates  $\mathcal{C} \setminus \mathbf{B}$  are lying on

bifurcation points, which enables the measurements of relative lengths and angles of bifurcations.

## 5 CONCLUSIONS AND FUTURE WORK

We have presented a set of methods for detecting particular landmarks from grape leaves, with a focus on the reconstruction of the venation network and the base point. Our method starts from an initial detection of segments in the image, which are then filtered based on the number of their intersections. The areas of intersections are clustered, each cluster being a candidate base point. The initial venation network being disconnected, we proposed a hill-climbing like algorithm for its reconstruction, resulting in a set of venation paths. Finally, the base point is selected as being the candidate from which the total length of the closest paths is maximal.

The proposed scheme detects the base point with an accuracy of 100% for the grape leaves database, and is robust to scale, orientation and contrast or illumination change. The main assumption being made is related to the palmate structure of the leaves, which induces a hierarchical venation network rooted on the base point. The landmark extraction is a preliminary yet necessary step toward a proper classification and identification of the leaves. We applied successfully the venation and base extraction on the palmate subset of a more general database. As future work, we can mention the classification of the leaves based on the morphometric features, by the joint use of the blade, the reconstructed venation network and the extracted landmarks. Also, the discriminative power and sensitivity of the descriptors against the number of varieties and the amount of data are of principal interest.

## ACKNOWLEDGEMENTS

This research has been conducted with the support of the Agropolis Foundation through the PI@ntNet project. The authors would also like to thank the members of the PI@ntGrape case study, and in particular Jean-Michel Boursiquot & Thierry Lacombe (INRA, UMR AGAP, DAVEM team), Thierry Dessup (INRA, Vassal Domain) and Christophe Sereno (INRA, UMR Amap).

## REFERENCES

- Comaniciu, D. and Meer, P. (2002). Mean shift: a robust approach toward feature space analysis. *IEEE Trans. on PAMI*, 24(5):603–619.
- Coutaud, M. et al. (2009). Advances in taxonomic identification by image recognition with the generic content-based image retrieval Ikona. In *e-Biosphere*.
- Levkowitz, H. and Herman, T. (1993). GLHS: A generalized Lightness, Hue, and Saturation color models. *CVGIP: Graphical Models and Image Processing*, 55(4):271–285.
- Nam, Y. et al. (2008). A similarity-based leaf image retrieval scheme: Joining shape and venation features. *Computer Vision and Image Understanding*, 110(2):245–259.
- OIV expert group “Vine selection” (2009). The OIV descriptor list for grape varieties and *Vitis* species. Technical report, International Organisation of Vine and Wine (OIV).
- Park, J.-K. et al. (2006). A venation-based leaf image classification scheme. In *Information Retrieval Technology*, volume 4182 of *LNCS*, pages 416–428. Springer.
- Soille, P. and Talbot, H. (2001). Directional morphological filtering. *IEEE Trans. on PAMI*, 23(11):1313–1329.
- Zana, F. and Klein, J. (2001). Segmentation of vessel-like patterns using mathematical morphology and curvature evaluation. *IEEE Transactions on Image Processing*, 10(7):1010–1019.